Reykjanes ambient noise reflection interferometry

Verdel, Arie; Wedemeijer, Harry; Paap, B; Vandeweijer, Vincent; Weemstra, Kees; Jousset, Philippe; Franke, Steven ; Blanck, Hanna; Águstsson, K.; Hersir, Gylfi Páll

Publication date
2016

Document Version
Final published version

Published in
European Geothermal Congress 2016

European Geothermal Congress 2016
Strasbourg, France, 19-24 Sept 2016

Reykjanes ambient noise reflection interferometry

Arie Verdel[1], Harry Wedemeijer[1], Bob Paap[1], Vincent Vandeweijer[1], Cornelis Weemstra[2], Philippe Jousset[3], Steven Franke[3], Hanna Blanck[4], Kristján Águstsson[4], Gylfi Páll Hersir[4]

[1] TNO, Utrecht, The Netherlands
[2] Delft University of Technology, Delft, The Netherlands
[3] GFZ, Potsdam, Germany
[4] ÍSOR, Reykjavik, Iceland

arie.verdel@tno.nl

Keywords: ambient noise, interferometry, reflection.

ABSTRACT

We present results from the application of ambient noise seismic interferometry (ANSI) to data that were recorded continuously in 2014 and 2015 at Iceland's peninsula Reykjanes. The objective of this study is the retrieval of reflected body waves (P-waves) that provide high-resolution velocity-versus-depth as well as subsurface structural information.

We show, for a subset of the onshore seismometers, that reflection information is present in the frequency bandwidth 3-8 Hz. We have observed both time-lapse variations where we expect them and time-invariant results where we do not expect to see changes.

As we lacked availability of active seismic reflection and well-sonic data that could serve as reference, we discovered, in our search to find a truly independent means for checking the reflection information quality of our ANSI results, that the coda of a global seismic P-wave, that is created by scattering in the crust, contains very high frequent (3-8 Hz) reflectivity information as it shows quite good correspondence with the 40-days ANSI results, whereas random noise correlation results, using the same amount of data as the coda response, shows less resemblance. We conclude that these results justify a more detailed investigation of the merits of the ANSI method for this data set.

But then, the ANSI-derived reflectivity estimates in turn clearly suggest that indeed P-wave crustal scattering information from global seismic waves is present in the frequency-range of 3–8 Hz, which is extremely high for global seismic waves. The latter aspect may open up a large range of opportunities for detailed crustal research at any location on the globe where broadband, and even short-period, seismometers are installed.

BACKGROUND

Crosscorrelating sufficiently long recordings of ambient noise by a pair of receivers allows one, in principle, to retrieve the Green's function (impulse response) between those two sensors (Derode et al. 2003, Wapenaar, 2004, Wapenaar and Fokkema, 2006). For seismic surface waves this was e.g. demonstrated by Shapiro and Campillo, 2004 and Shapiro et al., 2005 and for seismic body waves by Draganov et al., 2007, 2009, 2013.

Applications of the underlying principle are not limited to seismology: an interdisciplinary review of the correlation properties of random wave fields is provided by Larose et al. (2006).

The practical feasibility of ANSI has created a large range of new passive seismic applications, both for industrial geophysical exploration and monitoring purposes such as in geothermal- or hydrocarbon reservoir delineation (Draganov et al., 2013), CO_2-sequestration monitoring (Boullenger et al., 2015) as well as for crustal imaging at a basin scale, see Campillo and Roux (2015) for a broad overview and a detailed description of the originating mechanisms of seismic noise. The tutorial paper on seismic interferometry by Wapenaar et al. (2010) provides a comprehensive description of underlying principles and application examples of seismic interferometry in general, including ANSI. An extensive overview of the theory related to crosscorrelation of ambient noise is provided by Boschi and Weemstra (2015).

Within the past decade, the surface wave retrieval from continuous ambient noise registrations has become almost common practice for earthquake seismologists, which can be seen from the rapidly growing amount of publications on this subject. The number of studies on reflected body wave retrieval with ANSI is however still quite limited, as the amplitudes of these reflections are generally two orders of magnitude lower than those of surface waves due to the spherical (point-source-) spreading of the former, whereas surface waves exhibit line-source spreading. In addition, the requirement of having an even directional distribution and a sufficient density of ambient noise sources is often not met and, last but not least, the knowledge of the tectonic mechanisms leading to these micro-seismic events within the studied subsurface volumes is still rather limited.

Nevertheless, as body-wave reflections can provide high-resolution subsurface images, the potential reward of this ANSI application can be high. The results described in the following were produced within the context of European Union funded research project IMAGE (Integrated Methods for Advanced Geothermal Exploration).

AMBIENT NOISE CROSSCORRELATIONS

For body wave retrieval from recorded ambient noise we use the relation (Wapenaar, 2004):

$$\{G_{p,q}(\mathbf{x}_A,\mathbf{x}_B,t)+G_{p,q}(\mathbf{x}_A,\mathbf{x}_B,-t)\}*a(t) \approx \sum_i^N v_p^i(\mathbf{x}_A,-t)*v_q^i(\mathbf{x}_B,t) \qquad (1)$$

Here $G_{p,q}(\mathbf{x}_A,\mathbf{x}_B,\pm t)$ represent the causal and time-reversed Green's tensors between positions $\mathbf{x}_A$ and $\mathbf{x}_B$, $v^i_{p(q)}$ represents the particle velocity component in the $x_{p(q)}$ direction (p,q = 1,2,3) of the i-th passive noise record, * denotes convolution, t denotes time and $a(t)$ concerns the autocorrelation of the source time function of the noise sources. The sum on the right-hand side is formed by stacking N crosscorrelated ambient-noise records (convolution with a time-reversed field is equivalent to correlation). Approximate equation (1) relates the two-point seismic impulse response to the stacked crosscorrelations of ambient noise recordings $v^i_{p(q)}(\mathbf{x}_{A(B)},t)$; it is the discrete version of a 3D boundary surface integral, see Wapenaar and Fokkema (2006) for details. Thereby, the noise sources are assumed to be mutually uncorrelated and illuminating the sensors equally from all directions. An irregular illumination, often for a large part due to an irregular distribution of sources in the subsurface (and for another part due to focusing or defocusing of P-waves due to large velocity gradients), leads to causal and time-reversed Green's functions not being equal to each other.

In many cases, the source distribution becomes more regular by stacking noise records over longer periods of time. The length of the recording period T has both a natural as well as a practical limit though: the natural bound is formed by the pace of dynamic processes in the subsurface in which certain material quantities themselves can be subject of investigation with ANSI in time-lapse studies. The practical limit is provided by the fact that the signal-to-noise ratio of retrieved information is proportional to $\sqrt{T}$, see Gerstoft et al. (2006).

We consider (1) to be acceptable as starting point for our purposes since we have access to sufficiently long continuous broadband data recordings and because noise sources often are at most weakly correlated.

AMBIENT NOISE AUTOCORRELATIONS

Approximate identity (1) can be considered as a 3D elastic wave extension, for noise, of a 1D formulation that was provided several decades earlier: in his pioneering 'daylight imaging' paper, Claerbout (1968) shows that the autocorrelation of the global plane-wave transmission response of a plane wave source underneath a plane-layered medium gives the global plane wave reflection response. The term 'global' refers to the incorporation, in the response, of all multiple reflections due to the layering in-between source and receiver; this constraint on source position can be relaxed in 2D and 3D, which is described, together with much more background on Claerbout's paper, in Wapenaar et al. (2010). Instead of 'global' in many cases 'total' is used: 'total reflection response' and 'total transmission response' represent the actual recordings that include all scattered waves (the coda).

Claerbout's result implies for noise that the zero-offset P-wave global reflection response $R(\mathbf{x},\mathbf{x},t)$ can be obtained from the autocorrelation and stacking of passive recordings for long periods of time, typically days or weeks. The requirement would then be that the lateral velocity variations in the subsurface are small and that uncorrelated noise sources illuminate the subsurface from below. Under these assumptions, single-station autocorrelations provide local 1D structural acoustic-contrast-versus-depth information as we can invert global reflections to acoustic impedance profiles. The resolution of those profiles depends on the frequency content of the noise sources.

If repeated for other periods of time, time-lapse variations of seismic global reflection amplitudes may additionally be retrieved. Such time-lapse variations can be due to both a change, with time, of the reflection coefficients themselves as well as the time-variant two-way travel times between layer boundaries; the latter would be the result of a change with time, within a layer, of seismic P-wave velocity as a result of a change, with time, in pore fluid. The ANSI reflection results could then be compared with other noise-based time-lapse results such as analysis based on surface wave coda correlations (Weemstra et al., 2016).

To make Claerbout's zero-offset result and the connection of it with (1) more intuitive, Figure 1 (inspired from Ruigrok, 2014) can be helpful. It shows a subset of rays in a laterally constant subsurface with a single reflector at depth. These rays, including both direct transmission arrivals and twice-reflected rays, arrive at a regular array of seismometers and partially coincide. These rays are all due to a single deep noise source. It is well known (Wapenaar, 2010) that overlapping rays cancel during the correlation process. Applying (1) leads to multi-offset virtual shot panels, with a virtual shot at one of the receiver locations, being identical, for primary reflected waves, to common-midpoint-panels (CMPs), as the paths of the

rays that remain after crosscorrelation are identical if we compare both types of panels. The CMP, in turn, is identical to a common-reflection-point-panel in a laterally homogeneous earth.

By additionally assuming small x/z (see Figure 1), crosscorrelations converge to autocorrelations giving rise to a resulting zero-offset global reflection response with reflection points positioned, for a laterally constant subsurface, exactly vertically beneath the seismometers. The discrete equivalent of it is provided by (2) whereby $\mathbf{x}_A$ and $\mathbf{x}_B$ coincide and crosscorrelation on the right-hand side of (1) reduces to autocorrelation:

$$\{R(\mathbf{x}_A,\mathbf{x}_A,t)+R(\mathbf{x}_A,\mathbf{x}_A,-t)\}*a(t) \approx \sum_i^N v_3^i(\mathbf{x}_A,-t)*v_3^i(\mathbf{x}_A,t) \qquad (2)$$

We restrict ourselves to use of the vertical component v_3^i of the measured particle velocities only, since (nearly) vertically incoming P-waves at the surface are polarized in the vertical direction. As long as noise sources from the deep subsurface generate those P-waves, the illumination issue that we normally encounter for noise crosscorrelations, does not play a role either (leading to the causal and anti-causal Green's functions being equal, which is indeed per definition the case for the autocorrelation function). Furthermore, we make the assumption that $a(t)$, the autocorrelation of the noise source-time function, is approximately constant within the frequency range 3-8 Hz that we use. Although this seems a severe restriction, previous studies (Draganov et al., 2007, 2009) have shown that we can obtain reasonably good information about the approximate locations of seismic reflectors up to a few km depth with this approach. We therefore neglect the autocorrelation results in the two-way-time range 0.0 - 0.4 sec (the time-window wherein the autocorrelated source time function plays a role) throughout this study.

But what happens if strongly dipping reflectors occur in the Reykjanes subsurface? In that case, the autocorrelation results still represent an approximate zero-offset response. The difficulty, however, is that, for this situation, the reflection point locations become highly dip- and depth-dependent and are not representative anymore for the subsurface directly underneath the station location. This complicates the interpretation of the autocorrelation results considerably, of course, especially if we have a sparse station network.
The level of spatial detail of publicly available hard velocity-contrast (viz. seismic reflector-) information from the Reykjanes subsurface and its offshore continuation to the southwest, can be seen in Figure 2. For the upper few km of Reykjanes, it shows an approximately laterally constant velocity model and at most a few strong reflectors.

We therefore decided that it is reasonable to apply the noise autocorrelation method (2) on data from stations at Reykjanes such that results from it provide clues with regard to one of the key questions raised by field operator HS Orka:

"Up to which depths do our geothermal reservoirs extend?"

FIELD DATA EXAMPLES

In this section, we present a few results of application of the ANSI method on Reykjanes station network data. We selected for these examples 5 from the 30 deployed onshore broadband 20 Trillium Compact Broadband seismometers (BB): stations LFE, RAR, SDV, GEV and BER, and one from the 10 short-period Mark L-4C seismometers (SP), KRV; their locations can be seen in Figure 7. More details about the various station networks that are employed in IMAGE can be found in Blanck et al., 2016 and Jousset et al., 2016.

The processing sequence roughly looks as follows:

1) Prior to autocorrelation and stacking, elementary data processing is applied first, including resampling and DC-removal.
2) After autocorrelation and stacking, a frequency-bandpass filter is applied using a zero-phase Ormsby bandpass filter with corner frequencies 2-3-8-10 Hz.
3) When compared with modelled data, spectral shaping (whitening) is applied.

Scenario Modelling

We start with discussing a result for station LFE, located approximately 7 km from the nearest coastline. It is compared with modelled data using full wave field point source modelling for several 1D subsurface velocity scenarios for the upper 4 km (we use the SIL model as basis, see Figure 3). Figure 4 shows Model 1, which most resembles the SIL model; Model 2 contains a low-velocity perturbation in layer 3 and Model 3 contains a high-velocity perturbation in layer 2. Figure 5 shows the result for station LFE after stacking 40 consecutive days of autocorrelated recorded noise (leftmost trace). The second trace from the left shows the same result but after spectral whitening such that it can be easily compared with modelled scenarios. It can be seen from a comparison with the third trace from the left that a velocity-depth model with a thick shallow high velocity layer (Model 3) better matches the station data than the results from the other two models shown. This type of velocity-depth information can be considered a useful local refinement of results from tomographic inversion (Jousset et al, 2016).

Time-Lapse Reflectivities

The next data example concerns a time-lapse result for broadband station RAR which is located on the very tip of Reykjanes peninsula overlying the producing geothermal field (also named Reykjanes), which belongs to the larger Volcanic system (named Reykjanes as well), see Figure 6 and Figure 7. A selection was made of three approximately 6-week periods within one year (April 2014 - February 2015) wherein an autocorrelation stack was produced within the frequency bandwidth of 3-8 Hz, see Figure 8.

Apart from the pre-correlation trace data plots, in the following, the vertical axis in trace data plots denotes two-way travel time in sec.

When comparing the three stacked results, which should be a measure of the total P-wave reflection response (viz. including multiples), we notice large changes around two-way travel times 0.5 - 0.6 sec. Taking an average P-wave velocity in the range 3600 – 4000 m/s for the depth interval 0 – 1100 m (the latter corresponds with injection depth), this would lead to a two-way-time interval 0.55 - .6 sec., which nicely matches the interval with large observed time-lapse changes. We indeed expect to see changes in reflectivity during this period as a result of fluid injection at this location (Weemstra et al., 2016) because the seismic layer-velocity of P-waves is affected by the replacement of pore fluid. A more quantitative interpretation of this result is hence considered justified.

The following example, Figure 9, shows the autocorrelation stacks for broadband station SDV, located very closely to the southern coastline (Figure 7) for the same three periods as we analysed for station RAR. This time, we see hardy any time-lapse changes, which is also according to expectations, as the subsurface underneath SDV is not expected to contain large amounts of migrating geothermal fluids since we are located here at the margin of the geothermal reservoir region. Notice also the much more low-frequent character of the SDV-autocorrelations as compared to the RAR-autocorrelations. On purpose, the autocorrelations of both stations are not whitened since we want to study the raw spectral character, viz. the noise structure, of the ANSI results. It appears, after comparison with other broadband stations, that RAR exhibits anomalously high-frequent ANSI-signal. This might be explained by the actual presence of production equipment (e.g. pumps) in the close vicinity of RAR. In a more detailed follow-up study, the spectral properties of such equipment-noise would be analysed in order to remove its effect on the ANSI result.

Comparison with Global Seismic Wave Scattering

The next step that we describe here concerns the comparison of the ANSI stacks with reflectivity estimates that are obtained via other means.

Unfortunately, no active seismic reflection data were available for our studies: apart from the coarse velocity profiles derived from the regional seismic lines shown in Figure 2 (Weir et al., 2001), no suitable reflection information could be identified. Also, in order to compute acoustic impedance-versus-depth profiles that are representative for the studied station locations, one would need to obtain sonic and density log information from neighbouring wells. Again, the availability of this type of information appeared rather limited: only one well was identified but the logging data did not exceed a depth larger than 1km.

Inspired by the success of published high-frequency crustal seismic scattering investigations (Earle and Shearer, 1998, Shearer and Earle, 2004, Ruigrok et al., 2012a, and Ruigrok et al., 2012b), it was decided to test a very optimistic idea:

What if there is useful reflection information in the 3-8 Hz range present in the coda of very strong global seismic events?

In the literature no examples could be found yet of studies that employ frequencies larger than 1 Hz for this purpose. So, as far as we know, this technique was most likely never applied before in this frequency range. Indeed, it seems rather unlikely that such high-frequent coda wave information would be caused such distant earthquakes, especially because of the presumed attenuation of those high frequencies along the very long travel paths through the mantle. On the other hand, if such scattered information indeed would be available, it would be extremely helpful for testing the value of our ANSI results for Reykjanes.

We believed that testing this adventurous idea would anyhow be worth the effort, for the following reason: if we would take an earthquake from the other side of the globe, the direct P-phase would arrive from below at the transition of upper mantle to lower crust (viz. the Moho) approximately as a plane wave, having a horizontal wave front. That means, that the body-wave travels approximately vertically and its travel direction would be even closer to vertical while it propagates in the crust because of the lower P-velocities in the crust as compared to the P-velocities in the upper mantle. In a nearly plane horizontally layered velocity scenario for the Reykjanes subsurface (Figure 2), it would be realistic that autocorrelations bring out the normally reflected energy (energy vertically scattered within the crust) from the global seismic wave.

That such type of information really *can* be retrieved can be seen from Figure 10. For station SDV, we now compare the ANSI result (left panel) with global seismic autocorrelated P-wave coda. The ANSI-trace

includes a correction for point-source spreading: this is done by multiplying trace-samples with P-wave travel distance D(t) that is computed using a station-specific vertical velocity model V(z). This ANSI result was produced for the period April-June 2014, a 40-day stack, see the panel of two identical traces on the left (traces are repeated just for convenience).

The panel in the middle represents the global seismic result. It concerns the autocorrelated and 3-8 Hz filtered result of 150 sec raw data around the P-phase from a very strong earthquake that occurred offshore Chile: Magnitude 8, Depth 10 km, time 23:46:45 UTC on April 1st 2014, see IRIS website. We refer to this earthquake in the sequel as the Chile event.

The recorded global seismic P-phase due to this large earthquake can be very clearly observed in Figure 11, between 20 to 60 sec arrival time after midnight on April 2nd, 2014, viz. approximately 13 min 35 sec – 14 min 15 sec after earthquake origin time (the first 150 sec of April 2nd 2014 is used for autocorrelation).

Notice that SP station KRV shows, in Figure 11, not surprisingly, a response that is largely different from the responses of the 4 BB stations shown: the direct P-phase cannot be discerned on KRV due to the wave's very low-frequent characteristics. After applying the 3-8 Hz filter, however, see Figure 12, comparable responses can be observed for all 5 stations (the low-frequent direct P-phase has disappeared).

Returning now to Figure 10, it can be seen from a comparison of the ANSI panel on the left with the autocorrelated 150 sec data window around the direct P-phase from the Chile earthquake (middle panel), that there is a good correspondence in a considerable depth range. This is confirmed if we compare the left panel (ANSI result) with the rightmost panel: the latter was produced by autocorrelating 150 sec noise that was recorded 12 hours after the Chile earthquake, such that coda information associated with it can be ignored.

The match of the panel on the right of Figure 10 with the ANSI-stacked result (left panel) is quite poor. The better correspondence, within a considerable two-way-time range, of the 40-days ANSI autocorrelation stack with the Chile-event correlation suggests that:

1) *The 40-days ANSI result contains indeed reflection information, and*
2) *The coda of the Chile event produced from scattering in the crust directly underneath station SDV provides reflection information at least in the depth range wherein it provides a good match with the ANSI-derived reflectivity.*

The same phenomenon can be observed, at slightly different depth intervals, on stations KRV (Figure 13), RAR, GEV and BER, see the complete overview of comparisons for the 5 employed stations in Figures 14 and 15.

With this highly unconventional approach of looking at P-wave scattering from a global seismic wave in the very high (3-8 Hz) frequency range, we have obtained a clear indication, even confirmation, that ANSI-derived reflectivity information can be produced in certain depth ranges at Reykjanes.

But then, the ANSI-derived reflectivity estimates clearly suggest that P-wave crustal scattering information from global seismic waves is present in the same frequency-range of 3 – 8 Hz, which is extremely high for global seismic wave-analysis standards. The latter aspect may open up a large range of opportunities for detailed crustal research at any location on the globe where broadband, and even short-period, seismometers are installed.

CONCLUSIONS AND OUTLOOK

We have shown that the application of ambient noise interferometry (ANSI) for reflection retrieval has the potential of reducing uncertainties in, for geothermal exploitation, relevant subsurface parameters, such as the spatial distribution of seismic velocity jumps.

We have observed both time-lapse variations where we expect them and time-invariant results where we do not expect to see changes.

The value of the reflectivity information produced with ANSI was tested in a very unconventional way, because neither well-data nor active seismic data were available: we employed data from a very strong earthquake at the other side of the globe to investigate P-wave crustal scattering information content. In our search to find a truly independent means for checking the reflection information quality of our ANSI results, we discovered that the coda of a global seismic P-wave, that is created by scattering of it in the crust, contains very high frequent (3 – 8 Hz) reflectivity information as it shows, in some depth intervals, quite a striking correspondence with the 40-days ANSI results. This aspect was further verified by comparing the 40-days ANSI-results for five stations with autocorrelation results of 150 sec ambient noise that does not contain coda waves. In that case, the correspondence indeed appeared to be quite poor.

This is good news for both the Reykjanes subsurface investigation study with the ANSI method as well as for shallow high resolution crustal seismic investigations in general whereby scattered global seismic P-wave data are used (massive amounts of the latter type of data have been collected).

We have to investigate the mechanism for creating such high frequent information in more detail, but for now, as working hypothesis we propose the following: a strong elastic contrast such as the Moho could act as secondary source as soon as it is encountered by the

direct P-wave. This secondary source would have spectral properties that are determined by the characteristics of the elastic impedance jump discontinuity as well as by the spectral properties of the direct P-wave. The well-known phenomenon of (periodic) wind-induced high-frequency noise that is generated at hard acoustic contrasts (buildings, ships etc.) might be, to some extent, analogous to the global P-phase scattering at the Moho.

Of course we intend to look more closely into this proposed scattering phenomenon as we consider it relevant with an eye to the mentioned use of high-frequent crustal scattering data caused by global P-waves.

We also believe that the here discussed results justify a more in-depth investigation with ANSI using the Reykjanes data: A logical extension of the current data processing scheme is to crosscorrelate station-pairs in this seismometer network: In order to improve the lateral resolution of the subsurface structure, thereby identifying non-zero-offset reflectivity in the pre-stack virtual source crosscorrelation panels, provides the opportunity to obtain subsurface reflectivity-versus depth-point information at locations in-between the seismic station positions. This has the potential of further reducing uncertainties in, for geothermal exploitation, relevant subsurface parameters, such as the spatial distribution of seismic velocity jumps.

ACKNOWLEDGEMENTS

The research leading to these results has received funding from the European Community's Seventh Framework Programme under grant agreement No. 608553 (Project IMAGE). Instruments for the IMAGE project were provided by the GIPP (Geophysical Instrumental Pool of Potsdam). The Seismic Unix open source software package was highly beneficial for this work. Also, the use of the seismic processing package Promax was of great help for the study of the field data.

REFERENCES

Blanck, H., Jousset, P., Ágústsson, K., Hersir, G.P. and Flóvenz Ó.G.: Analysis of seismological data on Reykjanes peninsula, Iceland, *Proceedings of the European Geothermal Congress 2016*, Extended abstract EGC, Strasbourg, France, (2016), paper #381.

Boschi, L., and Weemstra, C.: Stationary-phase integrals in the cross-correlation of ambient noise, *Rev. Geophys*., 53, (2015), 411–451, doi:10.1002/2014RG000455.

Boullenger, B., Verdel, A., Paap, B., Thorbecke, J., and Draganov, D.: Studying CO2 storage with ambient-noise seismic interferometry: A combined numerical feasibility study and field-data example for Ketzin, Germany, *Geophysics*, 80(1), (2015), Q1-Q13, doi: 10.1190/geo2014-0181.1.

Campillo, M., and Roux, P.: 1.12 Crust and Lithospheric Structure - Seismic Imaging and Monitoring with Ambient Noise Correlations, Treatise on Geophysics (Second Edition) ,Vol. 1, Deep Earth Seismology, 391-417, *Elsevier*, (2015), doi:10.1016/B978-0-444-53802-4.00024-5.

Claerbout, J. F.: Synthesis of a layered medium from its acoustic transmission response, *Geophysics*, 33, (1968), 264–269, doi: 10.1190/1.1439927.

Derode, A., Larose, E., Tanter, M., de Rosny, J., Tourin, A., Campillo, M., & Fink, M. : Recovering the Green's function from field-field correlations in an open scattering medium (L), Journal of the Acoustical Society of America, 113(6), (2003), 2973–2976.

Draganov, D., Wapenaar, K., Mulder, W., Singer, J., and Verdel, A.: Retrieval of reflections from seismic background-noise measurements, *Geophysical Research Letters*, 34, (2007), L04305, doi: 10.1029/2006GL028735.

Draganov, D., Campman, X., Thorbecke, J., Verdel, A., and Wapenaar, K.: Reflection images from ambient seismic noise, *Geophysics*, Vol. 74, no. 5, (2009), A63-A67, doi: 10.1190/1.3193529.

Draganov, D., Campman, X., Thorbecke, J., Verdel, A. and Wapenaar, K.: Seismic exploration-scale velocities and structure from ambient seismic noise (> 1 Hz), *Journal of Geophysical Research: Solid Earth*, Vol. 118, (2013), 1-16, doi:10.1002/jgrb.50339.

Earle, P., and Shearer, P.: Observations of high-frequency scattered energy associated with the core phase PKKP, *Geophysical Research Letters*, 25, No. 3, (1998), 405-408, paper number 97GL53365.

Gerstoft, P., Sabra, K., Roux, P., Kuperman, W., and Fehler, M.: Green's functions extraction and surface-wave tomography from microseisms in southern California, *Geophysics*, 71(4), (2006), SI23-SI31, doi: 10.1190/1.2210607.

Jousset, P., Blanck, H., Franke, S., Agustsson, K., Metz, M., Ryberg, T., Hersir, G., Weemstra, C., Verdel, A., Bruhn, D.: Seismic tomography of Reykjanes, SW Iceland, *Proceedings of the European Geothermal Congress 2016*, Strasbourg, France, (2016), paper #281.

Larose, E., Margerin, L., Derode, A., van Tiggelen, B., Campillo, M., Shapiro, N., Paul, A., Stehly, L., and Tanter, M.: Correlation of random

wavefields: An interdisciplinary review: *Geophysics*, 71, no. 4, (2006), SI11–SI21, doi: 10.1190/1.2213356.

Ruigrok, E. and Wapenaar, K.: Global-phase seismic interferometry unveils P-wave reflectivity below the Himalayas and Tibet, *Geophysical Research Letters*, *39*, (2012a), L11303, doi:10.1029/2012GL051672.

Ruigrok, E., Campman, X., and Wapenaar, K.: Basin delineation with a 40-hour passive seismic record, *Bulletin of the Seismological Society of America*, 102, (2012b), 2165-2176, doi:10.1785/0120110242.

Ruigrok, E.: Receiver-pair seismic interferometry applied to body-wave USArray data, *Geophysical Journal International*, 198, (2014), 895-905, doi: 10.1093/gji/ggu168.

Shapiro, N., and Campillo, M.: Emergence of broadband Rayleigh waves from correlations of the ambient seismic noise, *Geophysical Research Letters*, 31, (2004), L07614, doi:10.1029/2004GL019491, 2004.

Shapiro, N., Campillo, M., Stehly, L., and Ritzwoller, M.: High resolution surface-wave tomography from ambient seismic noise: *Science*, 307, (2005), 1615–1618.

Shearer, P., and Earle, P.: The global short-period wavefield modelled with a Monte Carlo seismic phonon method, *Geophysical Journal International*, 158, (2004), 1103-1117, doi: 10.1111/j.1365-246X.2004.02378.x.

Tryggvason, A., Rögnvaldsson, S., and Flóvenz, Ó.: Three-dimensional imaging of the P-and S-wave velocity structure and earthquake locations beneath Southwest Iceland, *Geophysical Journal International*, 151, (2002), 848–866, doi: 10.1046/j.1365-246X.2002.01812.x.

Wapenaar, K.: Retrieving the elastodynamic Green's function of an arbitrary inhomogeneous medium by cross correlation, *Phys. Rev. Lett.*, Vol. 93 (25), (2004), 254301, doi: 10.1103/PhysRevLett.93.254301.

Wapenaar, K., and Fokkema, J.: Green's function representations for seismic interferometry, *Geophysics*, 71(4), (2006), SI33-SI46, doi: 10.1190/1.2213955.

Wapenaar, K., Draganov, D., Snieder, R., Campman, X., and Verdel, A.: Tutorial on seismic interferometry: Part 1 — Basic principles and applications, *Geophysics*, 75(5), (2010), 75A195-75A209, doi: 10.1190/1.3457445.

Weemstra, C., Obermann, A., Verdel, A., Paap, B., Blanck, H., Guðnason, E., Hersir, G., Jousset, P., and Sigurðsson, A.: Time-lapse seismic imaging of the Reykjanes geothermal reservoir, *Proceedings of the European Geothermal Congress 2016*, Strasbourg, France, (2016), paper #207.

Weir, N., White, R., Brandsdóttir, B., Einarsson, P., Shimamura, H., Shiobara, H., and the RISE Fieldwork Team: Crustal structure of the northern Reykjanes Ridge and Reykjanes Peninsula, southwest Iceland, *J. Geophys. Res.*, 106 (B4), (2001), 6347–6368, doi:10.1029/2000JB900358.

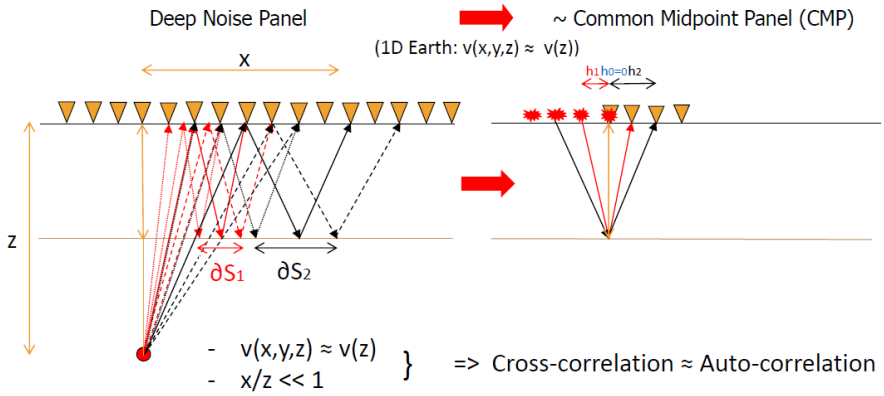

Figure 1: Reflected-wave ANSI with deep noise sources.

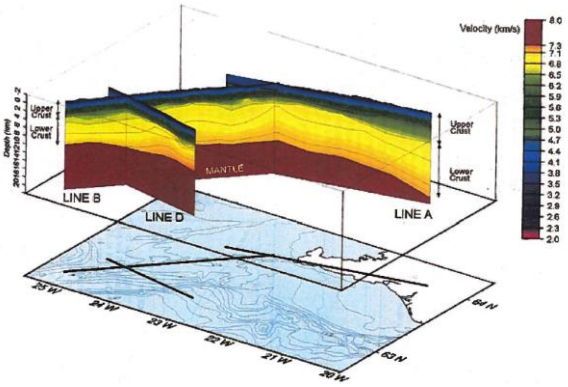

Figure 2: Crustal velocity profiles derived from the Reykjanes-Iceland Seismic Experiment (RISE) of 1996 (Weir et al., 2001).

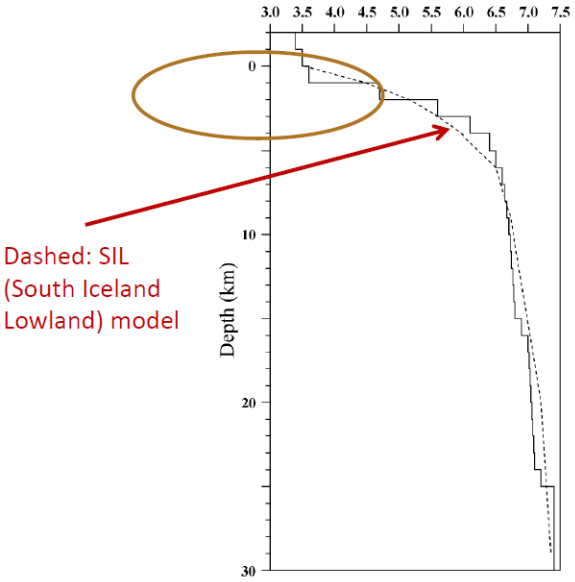

Figure 3: A small high-quality subset of local earthquake data was inverted to derive an initial 1-D layered *P*-velocity versus depth model (solid line), see Tryggvason et al. (2002) for more details.

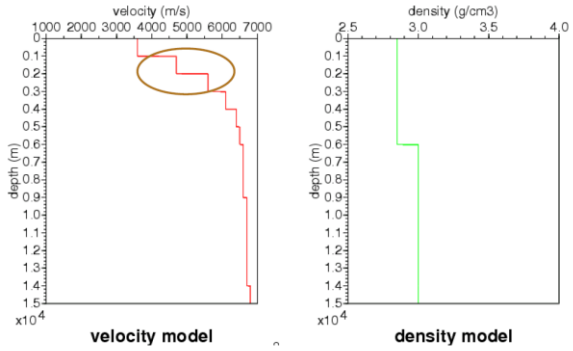

Figure 4: Model 1 that is used as basis for scenario modelling.

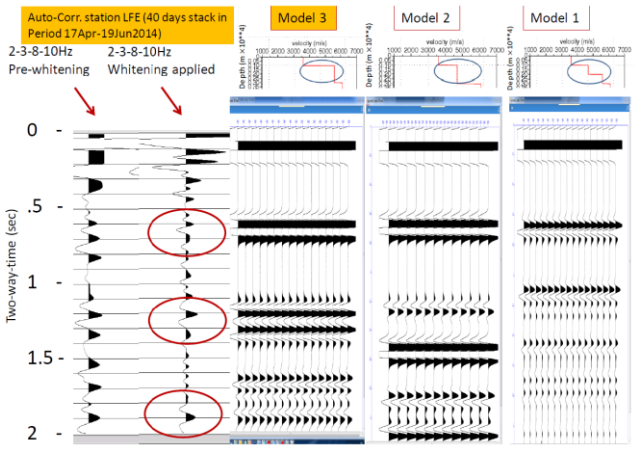

Figure 5: ANSI-processed autocorrelation stack for station LFE (two traces on left) and modelled global reflections for three velocity scenarios (modelled traces are repeated for convenience). Notice the encouraging match between the whitened field data result and the result computed for Model 3.

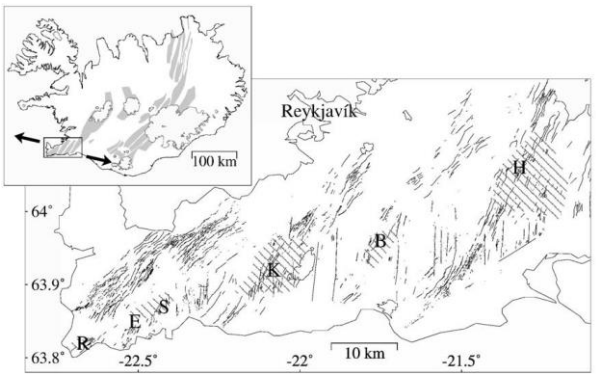

Figure 6: Tectonic map of Reykjanes peninsula, showing fracture locations and the locations of high-temperature geothermal fields, labelled as R: Reykjanes, E: Eldvörp, S: Svartsengi, K: Krísuvík, B: Brennisteinsfjöll and H: Hengill (from Keiding et al., 2010). Our study focuses around the fields R, E and S.

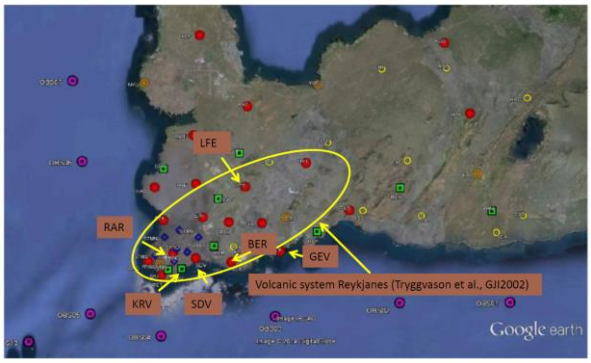

Figure 7: Map of part of Reykjanes peninsula, with the locations of the 6 seismometer stations that we used.

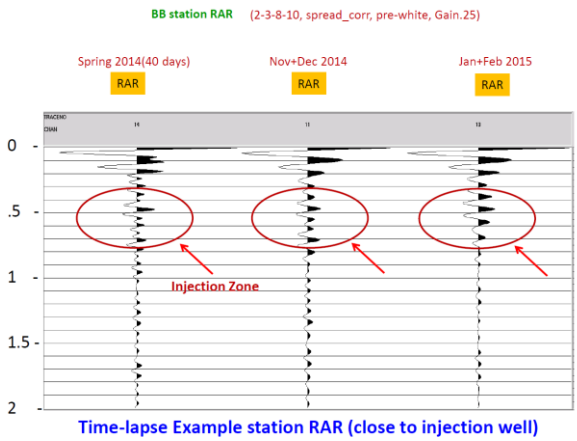

Figure 8: Time-lapse ANSI example BB station RAR (close to injection well). For 3 periods within one year, ~ 6 weeks of noise were correlated and stacked. We observe changes at the injection depth ~1100 m (0.55 - 0.6 sec two-way-time) due to fluid replacement.

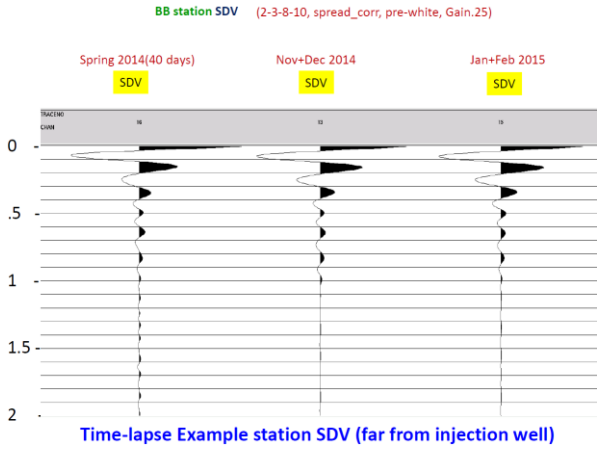

Figure 9: Time-lapse ANSI example BB station SDV (far from injection well). We see hardly changes occurring, as expected.

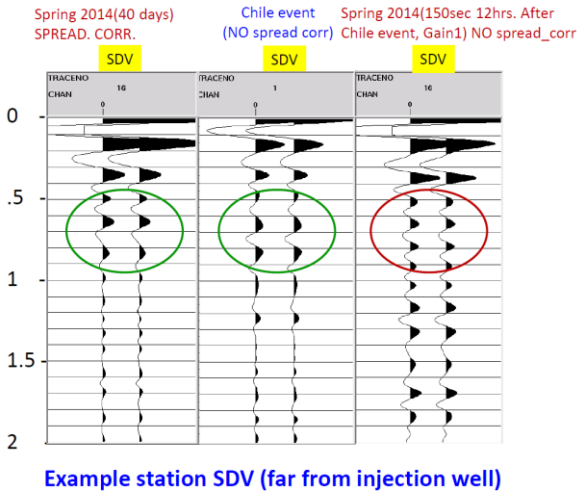

Figure 10: ANSI result (left) compared with the autocorrelated P-phase of the Chile earthquake using 150 sec data around the P-phase (middle) and the autocorrelated noise (150 sec) 12 hrs. after the earthquake (right). Notice the ANSI result is spherical spreading-corrected to allow a proper comparison to be made with the approximate plane wave scattering of Chile event. Green ellipses indicate a good correspondence with another panel. Red ellipse indicates a poor match with the other two panels in the same two-way-time (depth) range.

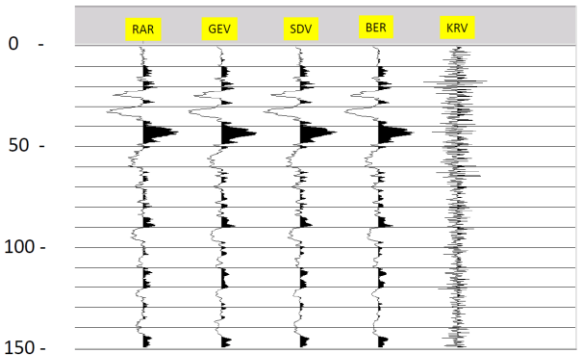

Figure 11: Raw recordings (150 sec) of 5 Reykjanes stations of P-phase (20-60 sec) of Chile earthquake (see text for details).

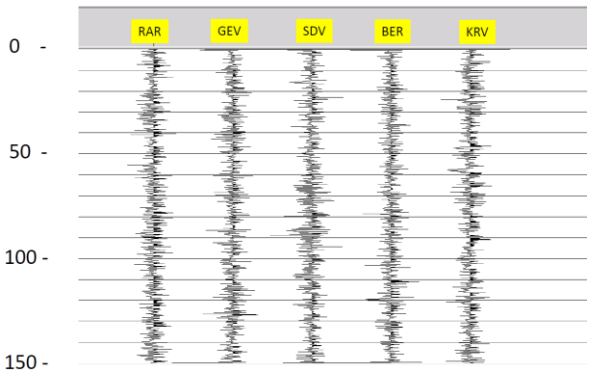

Figure 12: Bandpass filtered recordings (3-8 Hz) of 5 Reykjanes stations including P-phase of Chile earthquake (see text for details).

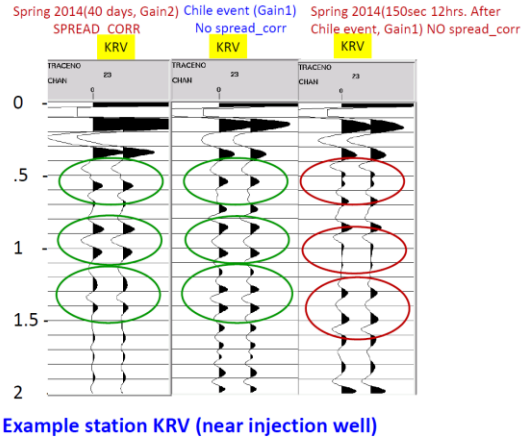

Figure 13: As in Figure 10, but now for SP station KRV. Green ellipses indicate a good correspondence with another panel. Red ellipses indicate a poor match with the other panels in the same time/depth range.

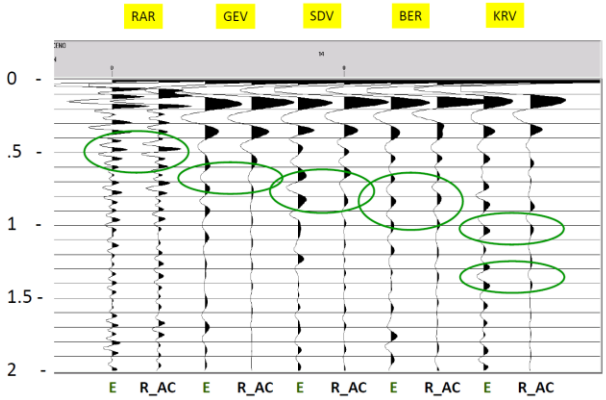

Figure 14: Comparison, for 5 Reykjanes stations (4 BB + 1 SP) of autocorrelated Chile earthquake recordings (150 sec around P-phase) E and the 40 days ANSI-stacked autocorrelated noise (R_AC). Notice the good correspondence within the green ellipses.

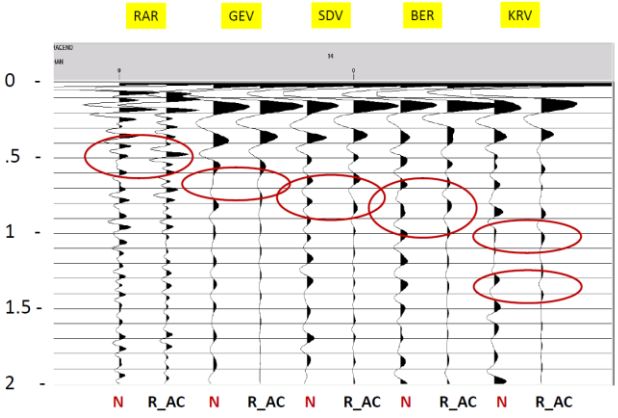

Figure 15: Comparison, for 5 Reykjanes stations (4 BB + 1 SP) of autocorrelated noise recordings N (150 sec) 12 hours after occurrence of the earthquake and the 40 days ANSI-stacked autocorrelated noise (R_AC). Notice the moderate correspondence within the red ellipses, as compared to Figure 14.